Results in Physics 41 (2022) 105924

Contents lists available at ScienceDirect

Results in Physics

journal homepage: www.elsevier.com/locate/rinp

Quantum memory and coherence dynamics of two dipole-coupled qubits interacting with two cavity fields under decoherence effect

A.-B.A. Mohamed [a,b,*,1], A.-H. Abdel-Aty [c,d,1], H. Eleuch [e,f,g,1]

[a] Department of Mathematics, College of Science and Humanities in Al-Aflaj, Prince Sattam bin Abdulaziz University, Al-Aflaj, Saudi Arabia
[b] Department of Mathematics, Faculty of Science, Assiut University, Assiut, Egypt
[c] Department of Physics, College of Sciences, University of Bisha, P.O. Box 344, Bisha 61922, Saudi Arabia
[d] Physics Department, Faculty of Science, Al-Azhar University, Assiut, 71524, Egypt
[e] Department of Applied Physics and Astronomy, University of Sharjah, Sharjah, United Arab Emirates
[f] College of Arts and Sciences, Abu Dhabi University, Abu Dhabi 59911, United Arab Emirates
[g] Institute for Quantum Science and Engineering, Texas A&M University, College Station, TX 77843, USA

ARTICLE INFO

Keywords:
Quantum-memory-assisted entropic uncertainty
Intrinsic decoherence
Entanglement

ABSTRACT

This paper investigates the intrinsic decoherence effect on quantum memory and coherence dynamics of two dipole-coupled qubits in a non-degenerate bimodel cavity. Entropic uncertainty, entropy, and concurrence are utilized to examine the dynamics of quantum-memory-assisted entropic uncertainty relations, mixedness, and entanglement. The results indicate that the nonlinear interactions between the two qubits and the cavity generate quantum-memory-assisted entropic uncertainty, mixedness, and entanglement, which are reliant not only on the qubit–qubit interaction but also on the intrinsic decoherence and coherence intensity of the initial two-mode cavity states. For specific values of the dipole–dipole interaction, non-classical correlations can be enhanced By reducing the initial intensity coherence, the stability of the quantum memory-assisted entropic uncertainty relations, as well as the two-qubit mixedness of the intrinsic decoherence, are accelerated.

Introduction

The uncertainty relations [1] are a fundamental concept in quantum physics. They illustrate how quantum physics differs from classical physics, as well as impose the lower bound on the precision for measuring two incompatible observables. The connection between the uncertainty relation and quantum information theory has been introduced and updated as the entropic uncertainty relations (EURs) for two arbitrary observables [2–4]. Teleportation [5], quantum key distribution [6], cryptographic security [7], and quantum metrology [8] are only a few of the possible uses for EURs. Here, EURs will be utilized to explore the dynamics of quantum-memory-assisted entropic uncertainty relations. The effects of the intrinsic decoherence, qubit–cavity and qubit–qubit interactions will be analyzed.

Quantum coherence [9–11], in particular purity and quantum entanglement [12], have striking features in many quantum information processing tasks, quantum information [13–15], quantum computation [16–19], teleportation [20], and quantum cryptography [21]. Tangles and von Newmann entropy have been shown to be reliable quantitative measures of entanglement in closed systems, and purity/mixedness in open systems [22]. In numerous physical quantum systems [23], entanglement of formation [24], concurrence [25], and negativity [26] have been proposed as suitable entanglement quantifiers. It is worth noting that Refs. [27,28] establish a link between coherence and quantum correlation.

The quantum memory-assisted entropic uncertainty relation (QM-A EUR) [29,30] is a key example of how the uncertainty relation and quantum correlation (between the quantum state of the observed system and the state of another quantum system (memory)) can be linked. QM-A EUR has been experimentally established [31–34]. Several research have confirmed the relationship between the uncertainty relation in quantum states and their entanglement (memory) using the uncertainty Alice-Bob procedure between two members (A and B qubits) [29,30]. Bob designates the two entangled qubits in this technique, and A-qubit is transferred to Alice as the measurement system, while B-qubit is rested with Bob as the memory system. Then, after collecting their measurements, Alice informs Bob of her decision. The two-qubit correlation/mixedness determines Bob's ability to predict Alice's

* Corresponding author at: Department of Mathematics, College of Science and Humanities in Al-Aflaj, Prince Sattam bin Abdulaziz University, Al-Aflaj, Saudi Arabia.
E-mail address: abdelbastm@yaoo.com (A.-B.A. Mohamed).
[1] All authors contributed equally to the manuscript preparation.

https://doi.org/10.1016/j.rinp.2022.105924
Received 24 April 2022; Received in revised form 12 August 2022; Accepted 15 August 2022
Available online 20 August 2022

outcomes. In several significant two-qubit systems, the relationship between quantum memory assisted entropic uncertainty and quantum correlations has been investigated, such as: Heisenberg XYZ chain with Dzyaloshinskii Moriya interactions [35], long-range two-qubit Ising model with an arbitrary magnetic field [36], three noninteracting qubits under a noisy environment [37], three Heisenberg-XXZ-chain qubits in a uniform magnetic field [38], and two dipole-coupled qubits subjected to a driving coherent radiation field [39].

Decoherence is a major issue in a growing number of quantum-processing-based technological applications [40]. Exploring its effects on the dynamics of quantum qubit information resources (especially intrinsic decoherence [41]) is therefore becoming a prominent objective in many practical qubit systems [42–44].

The motivation behind this publication is that (1) quantum systems cannot be completely shielded from decoherence since quantum memory and coherence are susceptible to decoherence effects. (2) There have been relatively few studies on the quantum memory and coherence dynamics of the two-qubit state that is created by qubit–cavity and qubit–qubit interactions [38]. Therefore, studying the dynamics of quantum-memory-assisted entropic uncertainty relations in the presence of generated qubit–qubit quantum coherence owing to qubit–cavity and qubit–qubit interactions under intrinsic decoherence is an exciting topic.

This manuscript is arranged as follows: In Section "The Model", an analytical description of the Milburn intrinsi c decoherence model for two qubits interacting with two-mode generalized coherent cavity fields is presented. Section "Two-qubit Information Resource Quantifiers" and Section "Dynamics of Two-qubit Effects" discuss the entropic uncertainty, two-qubit mixedness, and two-qubit concurrence dynamics. The conclusion is presented in Section "Conclusion".

The model

The considered physical system consists of two dipole-coupled qubits, that are coupled via the dipole–dipole interaction. Each j-qubit ($j = A, B$) includes the $|0_j\rangle$ lower and $|1_j\rangle$ upper energy states interact with bimodal cavity fields through a non-degenerate two-photon transitions. The Hamiltonian of the qubit–cavity interactions is given by

$$\hat{H} = \sum_{i=1}^{2} M_C^i + \sum_{j=A,B} M_{QC}^j + \hat{M}_{Qs}, \tag{1}$$

where the first term, $M_C^i = \omega_i(\hat{\psi}_i^\dagger \hat{\psi}_i + \frac{1}{2})$, represents the free Hamiltonians of the bimodal cavity fields. $\hat{\psi}_i^\dagger(\hat{\psi}_i)$ and ω_i ($i = 1, 2$) are the creation (annihilation) operators $\hat{\psi}_i^\dagger(\hat{\psi}_i)$ and the frequencies of the bimodal cavity fields, respectively. While the second and third terms, M_{QC}^j and $\hat{M}_{Qs}$, describe the interactions of the j-qubit with the bimodal cavity fields and the interactions between the two qubits, respectively. M_{QC}^j and $\hat{M}_{Qs}$ are given by

$$\begin{aligned} M_{QC}^j &= \frac{\omega}{2}\hat{\sigma}_z^j + \lambda(\hat{\psi}_1\hat{\psi}_2\hat{\sigma}_+^j + \hat{\psi}_1^\dagger\hat{\psi}_2^\dagger\hat{\sigma}_-^j), \\ \hat{M}_{Qs} &= J(\hat{\sigma}_+^A\hat{\sigma}_-^B + \hat{\sigma}_-^A\hat{\sigma}_+^B). \end{aligned}$$

Here, the two dipole-coupled qubits have the same frequency ω with the Pauli operators $\hat{\sigma}_+^j = |1_j\rangle\langle 0_j|$, $\hat{\sigma}_-^j = |0_j\rangle\langle 1_j|$, and $\hat{\sigma}_+^j = |1_j\rangle\langle 1_j| - |0_j\rangle\langle 0_j|$. The strength of the qubit–field interactions is controlled by the same coupling constant λ and the qubit–qubit coupling J.

We derive the Hamiltonian of Eq. (1) by transforming the operators of the two-mode cavity fields to Su(1, 1) operators, which provides an analytical description for the dynamics of the qubit–cavity. Due to the frequencies of the two-mode cavity fields are physically considerably less than the frequency between the qubit's two electronic levels and to generate Su(1, 1) operators, we take the case where the frequencies of the two-mode cavity fields are equal to half of the qubit-frequency, i.e., $\omega_1 = \omega_2 = \frac{\omega}{2}$. Thus, the qubit–cavity Hamiltonian of Eq. (1) by using the Su(1, 1) operators, $\hat{K}_\pm$ and $\hat{K}_0$ can be expressed as

$$\hat{H}_K = \omega K_o + \sum_{j=A,B} \frac{\omega}{2}\hat{\sigma}_z^j + \lambda(K_-\sigma_+^j + K_+\hat{\sigma}_-^i) + \hat{M}_{Qs}, \tag{2}$$

where, $\hat{K}_- = \hat{\psi}_1\hat{\psi}_2 = \hat{K}^\dagger{}_+$, $\hat{K}_0 = \frac{1}{2}(\hat{\psi}_1^\dagger\hat{\psi}_1 + \hat{\psi}_2^\dagger\hat{\psi}_2 + 1)$, $[\hat{K}_0, \hat{K}_\pm] = \pm\hat{K}_\pm$, and $[\hat{K}_-, \hat{K}_+] = 2\hat{K}_0$. These Su(1, 1) operators $\hat{K}_\pm$ and $\hat{K}_0$ (with the Bargmann number k) verify [45]:

$$\begin{aligned} \hat{K}_0|m,k\rangle &= (m+k)|m,k\rangle, \ \hat{K}_-|m,k\rangle = X_{k,m}|m-1,k\rangle \\ \hat{K}_+|m,k\rangle &= X_{k,m+1}|m+1,k\rangle, X_{k,m} = \sqrt{m^2+2km-m}. \end{aligned}$$

In the space qubit–cavity states $\{ |\varphi_1\rangle = |1_A 1_B, n, k\rangle, |\varphi_2\rangle = |1_A 0_B, n+1, k\rangle, |\varphi_3\rangle = |0_A 1_B, n+1, k\rangle, |\varphi_4\rangle = |0_A 0_B, n+2, k\rangle \}$, the eigenstates $|\Psi_i^n\rangle$ of the qubit–cavity Hamiltonian of Eq. (2) are given by

$$|E_m^n\rangle = \sum_{k=1}^{4} E_{mk}|\varphi_k\rangle, (m = 1, 2, 3, 4). \tag{3}$$

The coefficients E_{mk} satisfy the eigenvalue-condition: $\hat{H}|E_m^n\rangle = E_m|E_m^n\rangle$. The corresponding eigenvalues E_m^n are:

$$\begin{aligned} E_1^n &= \omega(n+k+1) \qquad E_2^n = \omega(n+k+1) - J, \\ E_3^n &= \omega(n+k+1) + \frac{1}{2}J - \frac{1}{2}\sqrt{J^2 + 8\lambda^2(X_{k,n+1}^2 + X_{k,n+2}^2)}, \\ E_4^n &= \omega(n+k+1) + \frac{1}{2}J + \frac{1}{2}\sqrt{J^2 + 8\lambda^2(X_{k,n+1}^2 + X_{k,n+2}^2)}. \end{aligned} \tag{4}$$

The decoherence can be described in a variety of approaches. One of these, intrinsic decoherence, which is regulated by the Milburn equation [41] and explains why the system loses its quantum coherence and entanglement as it progresses. For intrinsic decoherence, which results in a quantum coherence loss without the usual decay-related energy loss, Milburn established a governing dynamical equation. Others approaches are governed by Master equations, describing system–reservoir interactions [46,47], which lead naturally to decoherence as the information is immediately lost after evolution. The Milburn equation that governs the time evolution of the qubit–cavity density matrix $M(t)$ under the effect of decoherence (identified by the intrinsic decoherence rate γ) can be written as:

$$\frac{d}{dt}M(t) = -i[\hat{H}, M] - \frac{\gamma}{2}[\hat{H}, [\hat{H}, M]], \tag{5}$$

Multiple quantum effects in various real systems, including superconducting circuits [43], polar-molecule states [44], single C_{60} solid state transistors [48], and trapped-ion systems [49], have been investigated using the Milburn approach.

To determine a particular solution for the qubit–cavity density matrix $\hat{M}(t)$ of Eq. (5), we consider that the initial reduced two-qubit density matrix describes the upper two-qubit state as: $\hat{M}^{AB}(0) = |1_A 1_B\rangle\langle 1_A 1_B|$. While the initial two-mode fields are described by the generalized coherent state [50] as

$$|\alpha, k\rangle = \sum_{m=0}^{\infty} F_m\,|m,k\rangle, \tag{6}$$

with

$$F_m = \sqrt{\frac{|\alpha|^{2k-1}}{I_{2k-1}(2|\alpha|)}}\frac{\alpha^m}{\sqrt{m!\Gamma(2k+m)}}.$$

The functions $\Gamma(x)$ and $I_\nu(x)$ represent the gamma and the modified Bessel functions. It is highly appropriate to consider the nonlinear generalized coherent state $|\alpha, k\rangle$ as the initial state for the cavity fields. This type of coherent state can be formulated in the SU(1, 1)-system basis $\{|n,k\rangle\}(n = 0, 1, \ldots)$. It is the generalized entangled pair coherent state [50]. The generalized coherent state can be implemented by magnetized homogeneous anisotropic $2D$-Dirac materials [51]. It has certain crucial special states; the even and odd coherent states can be obtained from $|\alpha, k\rangle$ by taking $k = \frac{1}{4}$ and $k = \frac{3}{4}$, respectively. The nonlinear coherent state $|\alpha, \frac{1}{2}\rangle$, which describes a nonlinear coherent state that can be realized as a stationary state of the trapped ions' center-of-mass motion [52] is another special state for $|\alpha, k\rangle$. The analytical solution of the Milburn Eq. (5) is given by [53]

$$M(t) = \sum_{k=0}^{\infty} \frac{(\gamma t)^k}{k!} D^k(t) M(0) D^{\dagger k}(t), \tag{7}$$

where $D^k(t) = H^k e^{-i\hat{H}t} e^{-\frac{1}{2}t\gamma \hat{H}^2}$, and $M(0)$ is the initial qubit–cavity density matrix, which is expressed by

$$M(0) = |1_A 1_B\rangle\langle 1_A 1_B| \otimes |\alpha, k\rangle\langle \alpha, k|, (l = 1, 2) \tag{8}$$

By utilizing the eigenvalues E_m^n $(k = 1-4)$ and the eigenstates $|E_m^n\rangle$ of the qubit–cavity Hamiltonian of Eq. (2), the solution of the Milburn equation is then:

$$\hat{M}(t) = \sum_{m,n=0} \sum_{k=1,3,4} F_m F_n^* \{S_{k1} |E_k^m\rangle\langle E_1^n| + S_{k3} |E_k^m\rangle\langle E_3^n| + S_{k4} |E_k^m\rangle\langle E_4^n|\}, \tag{9}$$

with

$$\begin{aligned} S_{11} &= E_{11}^m E_{11}^n D_{11}, \quad S_{31} = E_{31}^m E_{11}^n D_{31}, \quad S_{41} = E_{41}^m E_{11}^n D_{41},\\ S_{13} &= E_{11}^m E_{31}^n D_{13}, \quad S_{33} = E_{31}^m E_{31}^n D_{33}, \quad S_{34} = E_{31}^m E_{41}^n D_{34},\\ S_{14} &= E_{11}^m E_{41}^n D_{14}, \quad S_{43} = E_{41}^m E_{31}^n D_{43}, \quad S_{44} = E_{41}^m E_{41}^n D_{44}, \end{aligned}$$

where the function $D_{r,s} = e^{-\frac{\gamma}{2}(E_r^m - E_s^n)^2 t}$ depends on the eigenvalues E_m^n of the Hamiltonian of Eq. (2). To explore quantum memory assisted entropic uncertainty and coherence dynamics for two qubits, we seek the temporal evolution of the reduced two-qubit density matrix $M^{AB}(t)$ by taking the trace over the states $\{|k\rangle\}(k = 0, 1, 2, \ldots, \infty)$ for the system density matrix $M(t)$ of Eq. (9).

$$M^{AB}(t) = \mathtt{tr}_{fields}\{M(t)\} = \sum_{k=0}^{\infty} \langle k|M(t)|k\rangle. \tag{10}$$

Two-qubit information resource quantifiers

- **Quantum-memory-assisted entropic uncertainty relations (QMA-EURs)**:
  Here, we consider the QMA-EURs derived by Berta et al. [54]. In the presence of quantum memory, the entropic uncertainty relations (for a pair of initially entangled state AB with the density matrix M_{AB}) are restricted by:

$$S(P|B) + S(Q|B) \geq S(A|B) + \log_2 \frac{1}{c}, \tag{11}$$

  where $S(A|B) = S(M_{AB}) - S(M_B)$ represents the density operator's conditional von Neumann entropy with the density matrix M_{AB}. $S(M) = -tr(M \log_2 M)$ designs the von Neumann entropy for a density matrix with $M \in \{M_{AB}, M_B\}$. $S(X|B) = S(M_{XB}) - S(M_B)$ with $X \in \{P, Q\}$ is the conditional Von Neumann entropy of the post measurement state M_{XB}:

$$M_{XB} = \sum_x (|\psi_x\rangle\langle\psi_x| \otimes \mathbf{I}) M_{AB} (|\psi_x\rangle\langle\psi_x| \otimes \mathbf{I}). \tag{12}$$

  Here $M_B = tr_A(M_{AB})$, $|\psi_x\rangle$ is the eigenvectors of X. $\mathbf{I}$ represents the identity operator. The parameter c on the right side of the inequality (11) is the maximal overlap of the observables P and Q. It is defined as: $c = \max_{ij} |\langle\phi_i \mid \varphi_j\rangle|^2$ with $|\phi_i\rangle$ and $|\varphi_i\rangle$ are the observable's eigenstates P and Q.
  In other words, the inequality (11) illustrates how the memory's effect reduce the lower bound of the memory-assisted entropic uncertainty relation.
  In the case of the two spins operators σ_x and σ_y, the left-hand and right-hand sides of the inequality (11) can be expressed as:

$$L(t) = S(M_{\sigma_x B}) + S(M_{\sigma_z B}) - 2S(M_B), \tag{13}$$

$$R(t) = S(M_{AB}) - S(M_B) + 1, \tag{14}$$

  $L(t)$ denotes the entropic uncertainty and $R(t)$ its lower bound.

- **Two-qubit concurrence entanglement (CE)** :
  One of the most popular quantifiers of entanglement between two particles A and B is the concurrence. It [55] can be used to explore the time-dependent two-qubit entanglement induced by qubit–cavity interactions. For the density matrix of the two particles $\hat{M}^{AB}(t)$. the expression of the concurrence is

$$C(t) = \max\{0, \sqrt{\lambda_1} - \sqrt{\lambda_2} - \sqrt{\lambda_3} - \sqrt{\lambda_4}\}, \tag{15}$$

  $\lambda_1 > \lambda_2 > \lambda_3 > \lambda_4$ represent the eigenvalues of the matrix: $R = \hat{M}^{AB}(\sigma_y \otimes \sigma_y)\hat{M}^{*AB}(\sigma_y \otimes \sigma_y)$.

- **Entropy mixednes (EM)** :
  Entropy is employed in this case to measure the amount of two-qubit mixedness [56,57]. The expression for qubit–qubit entropy is as follows:

$$S(t) = -\sum_{i=1}^{\infty} \lambda^i \ \ln(\lambda^i), \tag{16}$$

  which depends on the eigenvalues λ^i of the qubit–qubit state $M^{AB}(t)$ of Eq. (10).

Dynamics of two-qubit effects

Here, we explore the dynamics of the entropic uncertainty, two-qubit mixedness, and two-qubit concurrence for an initial generalized coherent cavity state. The Bargmann index is taken here as $k = \frac{1}{2}$.

In Fig. 1, $L(t)$, $R(t)$, $S(t)$, and $C(t)$ are plotted for different intrinsic decoherence rates with a large value ($\alpha = 6$). In the absence of the intrinsic decoherence and the dipole–dipole interaction, Fig. 1a depicts; (1) the dynamics of the quantum-memory-assisted entropic uncertainty procedure, in which Bob sends Alice an A-qubit that is initially disentangled (pure state) with another of his quantum memory B-qubits, i.e., the dynamics of Bob's ability to minimize his uncertainty about Alice's measurement outcomes in the absence of intrinsic decoherence and dipole–dipole interaction. Because Bob has access to the quantum memory B-qubit, the entropic uncertainty function $L(t)$ measures Bob's entire amount of ignorance about the outcome of Alice's measurement. (2) The dynamics of the two-qubit entropy mixedness, and concurrence, which are good indicator to the amount of the quantum memory B-qubit and the prediction accuracy of outcomes of Alice's measurement. (3) Nonlinear qubit–cavity interactions' capacity to produce two-qubit QMA-EURs, two-qubit entropy mixedness, and concurrence. We note that the inequality of the quantum-memory-assisted entropic uncertainty relations is indeed fulfilled, as shown in Fig. 1a. After the qubit–cavity interactions are started, the two-qubit quantifiers of the QMA-EURs, EM, and CE arise with periodic oscillatory behavior with π-period. This means that, due to the nonlinear cavity–qubit interactions, the initial pure excited two-qubit states (with no quantum-memory) can be evolved to correlated states. The dynamical behavior of the QMA-EURs relates to generating an irregular prediction accuracy of Alice's measurement results with these generated mixedness and entanglement. The oscillating behaviors of QMA-EURs and entropy mixednes dynamics are reverse to that of two-qubit entanglement. The increase in two-qubit mixedness enhances entropic uncertainty. The concurrence exhibits sudden birth and sudden death entanglement [58,59]. During the intervals where the entanglement is vanished (in which, the quantum memory B-qubit is completely erased), the generated QMA-EURs, two-qubit entropy mixedness reach their maxima. The gap between the entropic uncertainty and its lower bound vanishes periodically at certain specific times (i.e., $L(t) \approx R(t)$). As a result, the effects of quantum memory regulate not just the lower bound but also the actual uncertainty, allowing Bob to precisely estimate Alice's measurement predictions.

Fig. 1b, illustrates the dynamics of the measuring uncertainty and the entropy mixednes as well as the concurrence under the effect of the intrinsic decoherence $\gamma = 0.01\lambda$. By comparing Fig. 1b and a, we observe that in the presence of intrinsic decoherence, the qubit–cavity

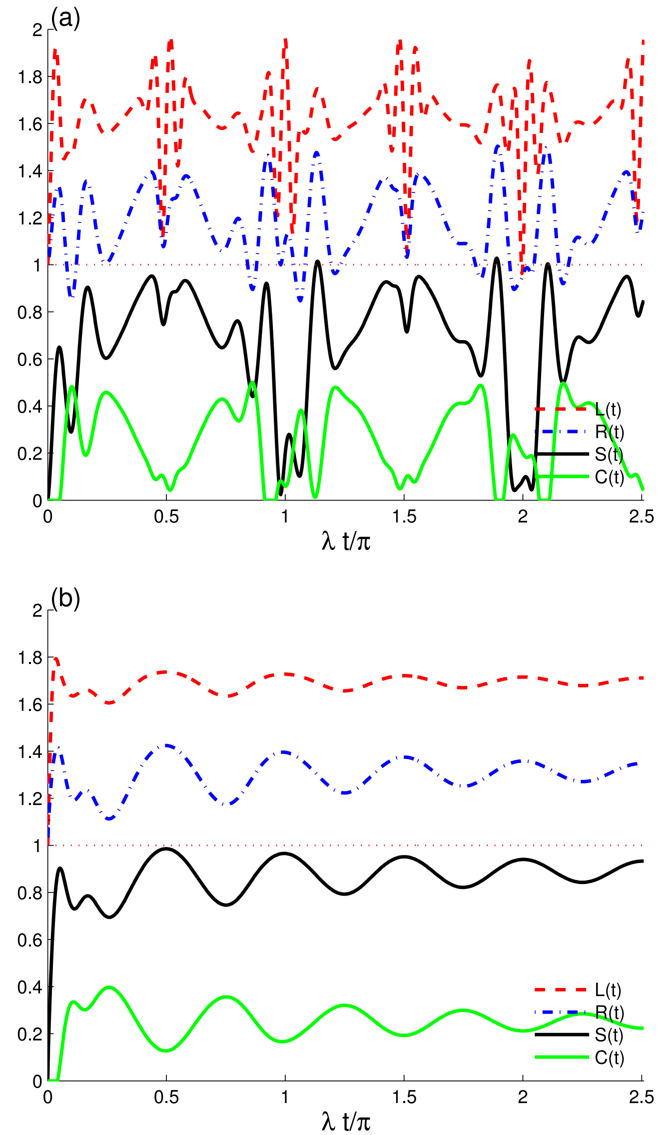

Fig. 1. Dynamics of the entropic uncertainty $L(t)$, its lower bound $R(t)$, entropy mixednes $S(t)$, and concurrence $C(t)$ are plotted when $\alpha = 6$ and $J = 0$ for different intrinsic decoherence rates: $\gamma = 0.0$ in (a) and $\gamma = 0.01\lambda$ in (b).

interactions are able to generate a stable quantum-memory-assisted entropic uncertainty, mixedness, and entanglement. The phenomena of two-qubit entanglement's sudden birth and death disappear. The stability of the generated partial two-qubit entanglement/quantum memory improves the stability of the Entropic uncertainty-relations. The lower bound of Alice's entropic uncertainty contains the same information as the two-qubit mixedness.

Fig. 2 illustrates the relation between the generated QMA-EURs, two-qubit mixedness, concurrence and the qubit–qubit interaction. The two-qubit measures are shown with the same values as in Fig. 1, but for different values of J/λ: $J = 5\lambda$ in (a), $J = 30\lambda$ in (b), and $J = 200\lambda$ in (c). From Fig. 2a and b, in the absence of the decoherence effect, we record following observations: (1) The oscillations and amplitudes of the QMA-EURs, two-qubit mixedness, and concurrence present notable changes. (2) QMA-EURs and two-qubit mixedness are reduced, while entanglement is enhanced. Furthermore, increasing the qubit–qubit interaction destroys the sudden birth–death two-qubit entanglement. Fig. 2c shows that increasing the strength of the qubit–qubit interaction leads to a reduction in quantum uncertainty with $L(t) \approx R(t)$, and an increase of the generated two-qubit entanglement/ quantum memory.

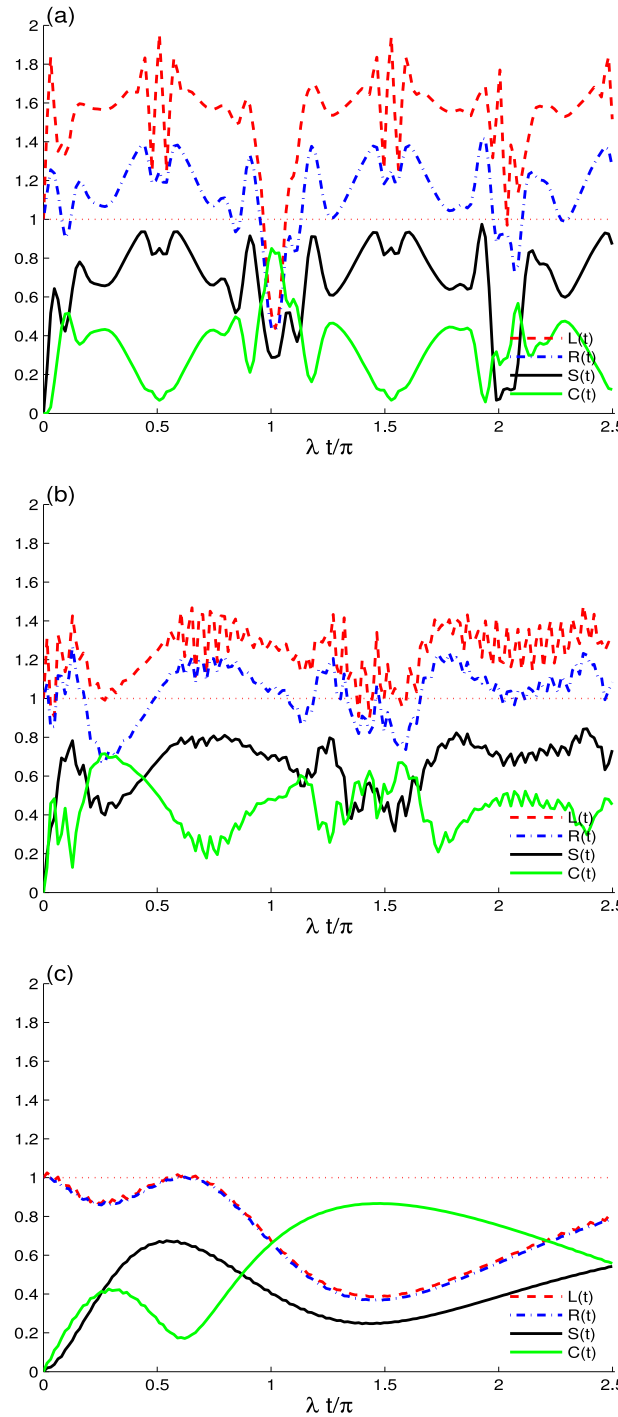

Fig. 2. Entropic uncertainty-relations, the entropy mixednes and the concurrence entanglement dynamics of Fig. 1a ($\gamma = 0.0$ and $\alpha = 6$) are plotted in the presence of the qubit–qubit interaction: $J = 5\lambda$ in (a), $J = 30\lambda$ in (b), and $J = 200\lambda$ in (c).

In this case of $L(t) \approx R(t)$, the quantum memory controls the lower limit and the uncertainty, allowing Bob to precisely estimate Alice's measurement predictions. We can deduce that the quantum memory increases as a result of the qubit–qubit interaction, and therefore the lower bound of the memory-assisted entropic uncertainty relations diminishes.

In Figs. 3 and 4, we examine how the dynamics of QMA-EURs, two-qubit mixedness, and two-qubit entanglement are affected by the dipole–dipole interaction. In Fig. 3, the QMA-EURs, EM, CE quantifiers

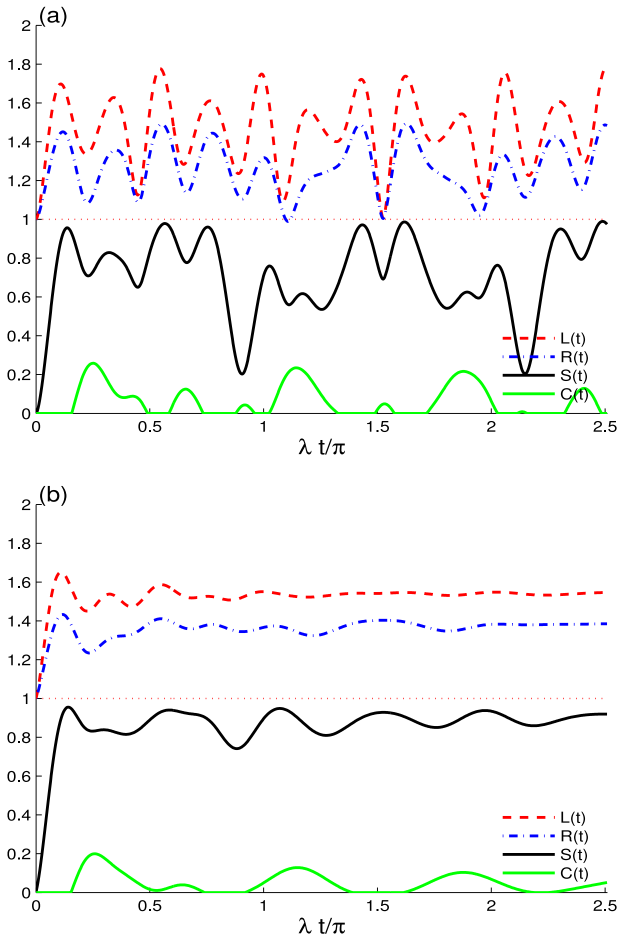

Fig. 3. Dynamics of the entropic uncertainty $L(t)$, its lower bound $R(t)$, entropy mixednes $S(t)$, and concurrence $C(t)$ are plotted for $J = 0$ and small value of the initial cavity coherence intensity $\alpha = 1$ for different intrinsic decoherence rates: $\gamma = 0.0$ in (a) and $\gamma = 0.01\lambda$ in (b).

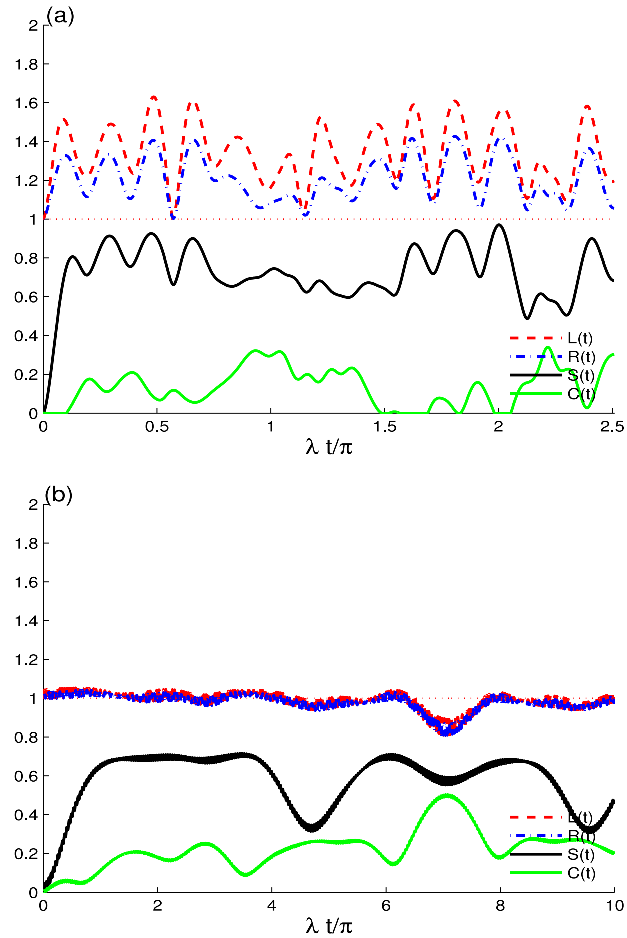

Fig. 4. The $L(t)$, $R(t)$ and $S(t)$ dynamics are depicted as Fig. 3a ($\gamma = 0.0$ and $\alpha = 1$) but for different values of J/λ: $J/\lambda = 5$ in (a) and $J/\lambda = 50$ in (b).

are depicted for a small value of the coherence intensity of the initial cavity state $\alpha = 1$ and different values' intrinsic-decoherence $\gamma/\lambda = 0.0$ in (a) and $\gamma/\lambda = 0.015$ in (b). To realize, the effects of the initial coherence intensity of the initial cavity state, we compare Fig. 1a with Fig. 3a. We find that, with a small value α, the nonlinear qubit–cavity interactions have a high ability to generate a strong two-qubit quantum uncertainty and entropy mixedness, and weaken entanglement. The sudden birth–death entanglement phenomena appear during several time intervals. Fig. 3b shows that, for a small initial value of the intensity coherence $\alpha = 1$ and for $J/\lambda = 0$, the intrinsic-decoherence has a plausible destructive effect on the generated qubit–qubit entanglement. The enhancement and stability of the QMA-EURs as well as the two-qubit mixedness of the intrinsic decoherence are accelerated by reducing the initial intensity coherence.

In Fig. 4, the QMA-EURs, EM, and CE quantifiers are depicted for a small value of the coherence intensity of the initial cavity state $\alpha = 1$ and qubit–qubit interaction J/λ: $J/\lambda = 5$ in (a) and $J/\lambda = 50$ in (b). In general the oscillatory behaviors of the QMA-EURs, EM, and CE quantifiers have notable changes in this case. The Fig. 4 results confirm the qubit–qubit interaction effects obtained with the condition with a large coherent field intensity $\alpha = 6$. The memory-assisted entropic uncertainty relations are more sensitive to dipole qubit–qubit interactions.

Conclusion

The interaction of two dipole-coupled qubits with a non-degenerate bimodal cavity is explored in this paper. The effects of initial intensity coherence, intrinsic decoherence, and dipole–dipole interaction on the dynamics of the quantum-memory-assisted entropic uncertainty relation, two-qubit mixedness, and two-qubit entanglement in the presence of intrinsic decoherence have been investigated. The results show that two-qubit mixedness is strongly related to the lower bound of entropic uncertainty, and they exhibit the same oscillatory behavior with different amplitudes, which is the reverse of two-qubit entanglement. The increase of the two-qubit mixedness improves entropic uncertainty, i.e., two-qubit entropy-mixedness has a significant impact on Alice-Bob measurement accuracy. We show that the initial intensity coherence, intrinsic decoherence, and dipole–dipole interaction all control the dynamics and generation of quantum memory-assisted entropic uncertainty, two-qubit mixedness, and two-qubit entanglement. The sudden birth and death entanglement phenomena is observed. In the presence of intrinsic decoherence, the qubit–cavity interactions provide stable behavior for quantum-memory-assisted entropic uncertainty, mixedness, and entanglement, with the entropic uncertainty being more stable and having the same information as the two-qubit mixedness. The sudden birth–death two-qubit entanglement vanishes. The increase of the dipole–dipole interaction can partially enhance the two-qubit entanglement/quantum memory, which leads to improved estimation of Bob'predictions of Alice's measurement. Our results indicate that the qubit–cavity and qubit–qubit interactions, as well as the intrinsic decoherence, have a significant impact on the precision of predicted measurements in quantum information processing. Entropic uncertainty is improved by the two-qubit entanglement and mixedness. The qubit–cavity interactions can provide stable quantum memory-aided entropic uncertainty, mixedness, and entanglement in the presence of intrinsic decoherence. Numerous quantum processing tasks, such as quantum key distribution [60], quantum cryptography [61], and entanglement witness [62], may benefit from the use of quantum-memory-assisted entropic uncertainty. In order to implement quantum computing [63,64] and qubit-channel metrology [65], stable mixedness and entanglement are needed.

Declaration of competing interest

The authors declare that they have no known competing financial interests or personal relationships that could have appeared to influence the work reported in this paper.

Data availability

No data was used for the research described in the article.

Acknowledgments

The authors are very grateful to the referees for their constructive remarks which have improved the manuscript. The authors extend their appreciation to the Deputyship for Research & Innovation, Ministry of Education in Saudi Arabia for funding this research work through the project number (IF-PSAU-2021/01/17712).

All authors approved the version of the manuscript to be published.

References

[1] Coles PJ, Berta M, Tomamichel M, Wehner S. Rev Modern Phys 2017;89:015002.
[2] Hertz A, Cerf NJ. J Phys A Math Theor 2019;52:173001.
[3] Bialynicki-Birula I. Phys Lett A 1984;103:253.
[4] Maassen H, Uffink JB. Phys Rev Lett 1988;60:1103.
[5] Hu ML, Fan H. Phys Rev A 2012;86:032338.
[6] Chen Z, Zhang Y, Wang X, Yu S, Guo H. Entropy 2019;21:652.
[7] Ng NHY, Berta M, Wehner S. Phys Rev A 2012;86:042315.
[8] Luis A, Rodil A. Phys Rev A 2013;87:034101.
[9] Ferreira DLB, Maciel TO, Vianna RO, Iemini F. Phys Rev B 2022;105:115145.
[10] Mohamed A-BA, Eleuch H. Eur Phys J Plus 2017;132(2):1–8.
[11] He Z, Han Z, Yuan J, Sinyukov AM, Eleuch H, Niu C, Zhang Z, Lou J, Hu J. Sci Adv 2019;5:763.
[12] Berrada K, Chafik A, Eleuch H, Hassouni Y. Quantum Inf Process 2010;9:13.
[13] Bennett CH, DiVincenzo DP, Smolin JA. Phys Rev A 1996;54:3824.
[14] Bose S, Knight PL, Plenio MB, Vedral V. Phys Rev Lett 1999;83:5158.
[15] Mohamed A-BA, Eleuch H. J Opt Soc Amer B 2018;35:47.
[16] Evangelisti S. Quantum correlations in field theory and integrable systems. Montreal: Minkowski Institute Press; 2013.
[17] Barenco A, Deutsch D, Ekert A, Jozsa R. Phys Rev Lett 1995;74:4083.
[18] Bengtsson I, Zyczkowski K. Geometry of quantum states: an introduction to quantum entanglement. Cambridge University Press; 2006.
[19] Sete EA, Eleuch H. Phys Rev A 2014;89:013841.
[20] Bennett CH, Brassard G, Crepeau C, Jozsa R, Peres A, Wootters WK. Phys Rev Lett 1993;70:1895.
[21] Ekert AK. Phys Rev Lett 1991;67:661.
[22] Mohamed A-BA, Eleuch H, Ooi CH. Phys Lett A 2019;383:125905.
[23] Mohamed A-BA, Eleuch H, Ooi CH. Sci Rep 2019;9:19632.
[24] Wootters WK. Phys Rev Lett 1998;80:2245.
[25] Hill S, Wootters WK. Phys Rev Lett 1997;78:5022.
[26] Dakic B, Vedral V, Brukner C. Phys Rev Lett 2010;105:190502.
[27] Yao Y, Xiao X, Ge L, Sun CP. Phys Rev A 2015;92:022112.
[28] Xi Z, Li Y, Fan H. Sci Rep 2015;5:10922.
[29] Renes JM, Boileau J-C. Phys Rev Lett 2009;103:020402.
[30] Berta M, Christandl M, Colbeck R, Renes JM, Renner R. Nat Phys 2010;6:659.
[31] Li CF, Xu JS, Xu XY, Li K, Guo GC. Nat Phys 2011;7:752.
[32] Prevedel R, Hamel DR, Colbeck R, Fisher K, Resch KJ. Nat Phys 2011;7:757.
[33] Demirel B, Sponar S, Abbott AA, Branciard C, Hasegawa Y. New J Phys 2019;21:013038.
[34] Sponar S, Danner A, Pecile V, Einsidler N, Demirel B, Hasegawa Y. Phys Rev Res 2021;3:023175.
[35] Zhang Y, Zhou Q, Fang M, Kang G, Li X. Quantum Inf Process 2018;17:326.
[36] Abdelghany RA, Mohamed A-BA, Tammam M, Obada A-SF. Quantum Inf Process 2020;19:392.
[37] Haddadi S, Pourkarimi MR, Wang D. J Opt Soc Am B 2021;38:2620.
[38] Abdelghany RA, Mohamed A-BA, Tammam M, Kuo W, Eleuch H. Sci Rep 2021;11:11830.
[39] Zhang Z-Y, Liu J-M. Physica A 2022;589:126639.
[40] Schlosshauer M. Decoherence and the quantum-to-classical transition. Berlin: Springer; 2008.
[41] Milburn GJ. Phys Rev A 1991;44:5401.
[42] Han J-X, Hu Y, Jin Y, Zhang G-F. J Chem Phys 2016;144:134308.
[43] Naveena P, Muthuganesan R, Chandrasekar VK. Physica A 2022;592:126852.
[44] Zhang Z-Y, Liu J-M. Sci Rep 2017;7:17822.
[45] Ban M. J Opt Soc Amer B 1993;10:1347.
[46] Kuang L-M, Tong Z-Y, Ouyang Z-W, Zeng H-S. Phys Rev A 1999;61:013608.
[47] Breuer H-P, Petruccione F. The theory of open quantum systems. Oxford University Press; 2002.
[48] Flores JC. Phys Lett A 2016;380:1063.
[49] Sharma SS, Sharma NK. J Opt B: Quantum Semiclass Opt 2005;7:230.
[50] Barut AO, Girardello L. Comm Math Phys 1971;21:41.
[51] Díaz-Bautista Y, Raya AJ. Phys: Condens Matter 2019;31:435702.
[52] de Matos Filho RL, Vogel W. Phys Rev A 1996;54:4560.
[53] Moya-Cessa H, Bužek V, Kim MS, Knight PL. Phys Rev A 1993;48:3900.
[54] Berta M, Christandl M, Colbeck R, Renes JM, Renner R. Nat Phys 2010;6:659.
[55] Bennett CH, Bernstein HJ, Popescu S, Schumacher B. Phys Rev A 1996;53:2046.
[56] Phoenix SJD, Knight PL. Phys Rev A 1991;44:6023.
[57] Bennett CH, Bernstein HJ, Popescu S, Schumacher B. Phys Rev A 1996;53:2046.
[58] Zyczkowski K, Horodecki P, Horodecki M, Horodecki R. Phys Rev A 2001;65:012101.
[59] Ficek Z, Tanaś R. Phys Rev A 2006;74:024304.
[60] Koashi M. New J Phys 2009;11:045018.
[61] Dupuis F, Fawzi O, Wehner S. IEEE Trans Inform Theory 2015;61:1093.
[62] Berta M, Coles PJ, Wehner S. Phys Rev A 2014;90:062127.
[63] Siomau M, Fritzsche S. Eur Phys J D 2011;62:449.
[64] Graham TM, Song Y, Scott J, Poole C, Phuttitarn L, Jooya K, Eichler P, Jiang X, Marra A, Grinkemeyer B, Kwon M, Ebert M, Cherek J, Lichtman MT, Gillette M, Gilbert J, Bowman D, Ballance T, Campbell C, Dahl ED, Crawford O, Blunt NS, Rogers B, Noel T, Saffman M. Nature 2022;604:457.
[65] Collins D. Phys Rev A 2019;99:012123.